AFRL-RX-WP-JA-2020-0309

A DIFFERENT PERSPECTIVE ON CHOLESTERIC LIQUID CRYSTALS REVEALS UNIQUE COLOR AND POLARIZATION CHANGES (POSTPRINT)

Matthew S. Mills, Dean R. Evans, Timothy J. Bunning, and Michael E. McConney

AFRL/RXAP

Kyung Min Lee and Vincent P. Tondiglia

Azimuth Corporation

2 August 2019
Interim Report

AIR FORCE RESEARCH LABORATORY
MATERIALS AND MANUFACTURING DIRECTORATE
WRIGHT-PATTERSON AIR FORCE BASE, OH 45433-7750
AIR FORCE MATERIEL COMMAND
UNITED STATES AIR FORCE

REPORT DOCUMENTATION PAGE

Form Approved
OMB No. 0704-0188

1. REPORT DATE *(DD-MM-YY)*	2. REPORT TYPE	3. DATES COVERED *(From - To)*
2 August 2019	Interim	2 January 2019 – 2 July 2019

4. TITLE AND SUBTITLE
A Different Perspective on Cholesteric Liquid Crystals Reveals Unique Color and Polarization Changes (Postprint)

5a. CONTRACT NUMBER
In House

5b. GRANT NUMBER

5c. PROGRAM ELEMENT NUMBER

6. AUTHOR(S)
Matthew S. Mills, Dean R. Evans, Timothy J. Bunning, and Michael E. McConney –
AFRL/RXAP
(Continued on next page)

5d. PROJECT NUMBER

5e. TASK NUMBER

5f. WORK UNIT NUMBER
X1SQ

7. PERFORMING ORGANIZATION NAME(S) AND ADDRESS(ES)
AFRL/RX
2977 Hobson Way (Continued on next page)
Wright-Patterson AFB OH 45433

8. PERFORMING ORGANIZATION REPORT NUMBER
1)

9. SPONSORING/MONITORING AGENCY NAME(S) AND ADDRESS(ES)
Air Force Research Laboratory
Materials and Manufacturing Directorate
Wright-Patterson Air Force Base, OH 45433-7750
Air Force Materiel Command
United States Air Force

10. SPONSORING/MONITORING AGENCY ACRONYM(S)
AFRL/RXAP

11. SPONSORING/MONITORING AGENCY REPORT NUMBER(S)
AFRL-RX-WP-JA-2020-0309

12. DISTRIBUTION/AVAILABILITY STATEMENT
DISTRIBUTION STATEMENT A. Approved for public release: distribution is unlimited.

13. SUPPLEMENTARY NOTES
PA Case Number: 88ABW-2019-3524; Clearance Date: 2 Aug 2019. This document contains color. Journal article published in ACS Applied Materials Interfaces, Vol. 12, No. 33, 16 Jul 2020, pp. 37400–37408. © 2020 American Chemical Society. The U.S. Government is joint author of the work and has the right to use, modify, reproduce, release, perform, display, or disclose the work. The final publication is available at https://doi.org/10.1021/acsami.0c09845

14. ABSTRACT ***(Maximum 200 words)***
Planar cholesteric liquid crystals (CLCs) are well known for having vibrant reflective coloration that is associated with the handedness and the pitch length of the helicoidal twist of the liquid crystalline molecules. If one observes these films at oblique angles, the reflected colors blue-shift with increasing angles from normal. On the other hand, uniform lying helix (ULH) CLCs, where the helicoidal axis lies in the plane of the substrate, are well-known but are not typically associated with vibrant colors. Here, we examine the unique optical properties of CLCs at oblique incidence angles, specifically the spectral and polarization changes associated with switching between planar and ULH CLCs for various incidence angles. At small angles of incidence ($0° < \psi < 45°$, where ψ is the angle of incidence relative to the surface normal at the substrate–CLC interface), the electrically driven helical reorientation from planar to ULH results in a blue-shifting of the color and circularly polarized to unpolarized switching behavior. At large angles ($45° < \psi < 90°$), the behavior is reversed, with a red-shifting color change occurring and the polarization switching from unpolarized to circularly polarized.

15. SUBJECT TERMS
cholesteric liquid crystals, uniform lying helix, total reflection, oblique incidence angle, circular polarization 3D display technology

16. SECURITY CLASSIFICATION OF:			17. LIMITATION OF ABSTRACT:	18. NUMBER OF PAGES	19a. NAME OF RESPONSIBLE PERSON (Monitor)
a. REPORT	b. ABSTRACT	c. THIS PAGE			Marc Martin
Unclassified	Unclassified	Unclassified	SAR	12	19b. TELEPHONE NUMBER *(Include Area Code)* (937) 255-9645

REPORT DOCUMENTATION PAGE Cont'd

6. AUTHOR(S)

Matthew S. Mills, Dean R. Evans, Timothy J. Bunning, and Michael E. McConney - AFRL/RXAP

Kyung Min Lee and Vincent P. Tondiglia - Azimuth Corporation

Victor Reshetnyak - Tara Shevchenko National University

.

7. PERFORMING ORGANIZATION NAME(S) AND ADDRESS(ES)

AFRL/RX
2977 Hobson Way
Wright-Patterson AFB OH 45433

Azimuth Corporation
4027 Colonel Glenn Hwy, Ste. 230
Beavercreek OH 45431

Tara Shevchenko National University of Kyiv
Theoretical Physics Department
Kyiv 01033 Ukraine

ACS APPLIED MATERIALS & INTERFACES

www.acsami.org Research Article

A Different Perspective on Cholesteric Liquid Crystals Reveals Unique Color and Polarization Changes

Kyung Min Lee, Mariacristina Rumi, Matthew S. Mills, Victor Reshetnyak, Dean R. Evans, Timothy J. Bunning, and Michael E. McConney*

Cite This: ACS Appl. Mater. Interfaces 2020, 12, 37400–37408 Read Online

ACCESS | Metrics & More | Article Recommendations | Supporting Information

ABSTRACT: Planar cholesteric liquid crystals (CLCs) are well known for having vibrant reflective coloration that is associated with the handedness and the pitch length of the helicoidal twist of the liquid crystalline molecules. If one observes these films at oblique angles, the reflected colors blue-shift with increasing angles from normal. On the other hand, uniform lying helix (ULH) CLCs, where the helicoidal axis lies in the plane of the substrate, are well-known but are not typically associated with vibrant colors. Here, we examine the unique optical properties of CLCs at oblique incidence angles, specifically the spectral and polarization changes associated with switching between planar and ULH CLCs for various incidence angles. At small angles of incidence ($0° < \psi < 45°$, where ψ is the angle of incidence relative to the surface normal at the substrate−CLC interface), the electrically driven helical reorientation from planar to ULH results in a blue-shifting of the color and circularly polarized to unpolarized switching behavior. At large angles ($45° < \psi < 90°$), the behavior is reversed, with a red-shifting color change occurring and the polarization switching from unpolarized to circularly polarized. Modeling of the light propagation through ULH CLCs is used to confirm the change in position and polarization characteristic of the reflection band with incidence angle observed experimentally. This study provides a new perspective on ULH CLCs and reveals a unique reconfigurable angular chromaticity.

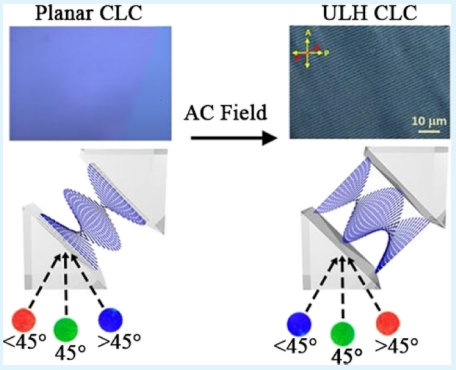

KEYWORDS: *cholesteric liquid crystals, uniform lying helix, total reflection, oblique incidence angle, circular polarization, 3D display technology*

INTRODUCTION

Our visual perception of our surroundings is a result of the complex interplay among our environment, light, our eyes, and our mind's interpretation of these received visual signals.[1] A defining characteristic of our visual perception that we share with other primates is our excellent stereoscopic acuity enabled by our binocular vision.[2] Immersive and realistic experiences can be created by taking advantage of our stereoscopic vision with three-dimensional (3D) display technologies that deliver slightly different information to each eye. Often, stereoscopic displays use unique eyewear to present each eye with the information representing our natural perspective, such as glasses with red/blue lenses for stereovisualization. Recently, movie theaters have employed polarization-based stereovisualization through the use of glasses with circular polarizers of opposite handedness for each eye. In addition to common two-dimensional liquid crystal displays, liquid crystals are also a common medium used to create 3D displays, such as commercial liquid crystal-based eyewear that exposes the eyes to differing perspectives on a temporal basis through a shuttering mechanism. Cholesteric liquid crystals (CLCs) are a liquid crystalline phase that offers unique characteristics for 3D visualization through the ability to separate light spectrally and based on polarization handedness.

CLCs self-assemble into periodic helicoidal arrangements that exhibit selective reflection, typically observed when the helical axis is perpendicular to the cell surface.[3−5] The spectral reflection associated with planar homogeneous CLCs probed orthogonal to the sample surface has a center wavelength given by $\lambda_B = \overline{n} \times P$, where $\overline{n}$ is the average refractive index and P is the pitch length of the CLC. The pitch length can be adjusted by controlling the concentration $[c]$ of chiral dopant molecules in an achiral nematic host through the following relationship: $P = 1/([c] \times \mathrm{HTP})$, where the helical twisting power, HTP, is a measure of the relative chiral dopant strength in twisting the nematic liquid crystalline host. When probed at near normal incidence angles, CLCs have a circularly polarized photonic

Received: May 29, 2020
Accepted: July 16, 2020
Published: July 16, 2020

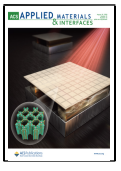

band gap associated with the handedness of the twisting direction of the CLC.

There have been numerous studies on the stimuli-responsive nature of the vivid colors in CLCs including spectral and efficiency changes in response to heat,[6−8] light,[9−14] and electrical[9,15−19] stimuli. There have also been many studies aimed at pushing the boundaries of the reflection contrast by affecting the reflection polarization.[8,20−25] The vast majority of this work involved using polymer stabilization of CLCs in the planar conformation, enabling CLC structures of opposite handedness to coexist in the same sample. An alternative approach is to exploit the intrinsic change in the polarization characteristics of the reflected light when the propagation direction is not along the helical axis.[26−30] As first reported by Fergason in 1966, greater than 50% reflectance can be achieved in planar CLCs at high angles of incidence with respect to the CLC helical axis.[26] Increasing the incidence angle of the planar CLC cell also shifts the reflection band to shorter wavelengths (blue tuning) according to the equation

$$\lambda_B(\theta) = \bar{n}P \cos\theta \quad (1)$$

where θ is the angle between the light propagation direction and the helical axis.[27−30] For a planar CLC, this angle is equivalent to the incidence angle measured in the liquid crystal (LC) medium, ψ: $\theta_P = \psi$, where the subscript P has been used to indicate the planar conformation (see Figure 1a). The reflectivity near the center of the band becomes larger than 50% for $\theta \approx 30°$, and it progressively increases with increasing incidence angles until almost complete reflection is observed at $\theta \gtrsim 60°$. This behavior can be seen in the schematic diagram and transmission spectra shown in Figure 2. As the planar CLC is tilted with respect to the direction of the probing light to an angle $\psi = \theta_P$ of up to 60°, there is a noticeable blue shift in the transmission notch from 1100 to 580 nm, consistent with eq 1. The unique feature seen in Figure 2 is the transition from circularly polarized reflection (~50% transmission) at angles near normal incidence to unpolarized reflection (>99% reflection) at high incidence angles. There have been several other theoretical and experimental explorations aimed at better understanding this angle-dependent spectral and polarization behavior.[31−36] At normal incidence, one of the two eigenmodes cannot propagate through the CLC medium and is reflected, while the other does not interact with the medium and is transmitted. At oblique incidence, both eigenmodes are diffracted by the medium to various extents. For large incidence angles, a region of total reflection is observed around $\lambda_B(\theta)$, together with regions of polarized reflection on the red and blue sides of $\lambda_B(\theta)$.[28,31,36] The width of the regions of unpolarized and circularly polarized reflection depends on the birefringence of the LC.[35] Recently, by exploiting the properties of planar CLCs with polymer stabilization at large incidence angles, we demonstrated a device with electrically tunable unpolarized reflection.[37]

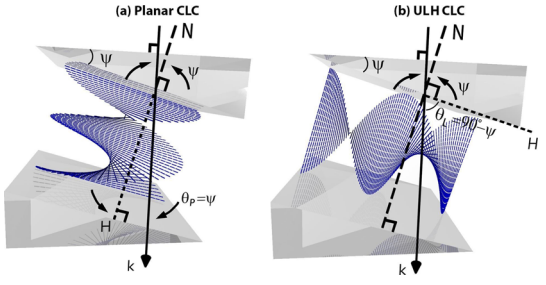

Figure 1. Diagram of relevant directions and angles for probing CLCs in the (a) planar or (b) ULH configuration: **k** = light propagation direction, **N** = normal to the CLC−glass interface, **H** = helical axis, ψ = angle between **k** and **N** (incidence angle at the CLC−glass interface), θ_P and θ_L = angle between **k** and **H** in the planar (subscript P) and ULH (subscript L) cases, respectively. **k**, **H**, and **N** are all in the same plane for cases (a,b).

All previous studies accessed the unpolarized reflection regime by tilting the glass cell substrates with respect to the incident light, as in the case of Figure 2. The alternative approach of changing the orientation of the CLC helix within the glass cell itself is not typically associated with vivid coloration and thus has not been fully explored. Achieving a short-pitch CLC with the helical axis tilted relative to the cell substrate has been demonstrated experimentally only very recently.[38,39] In these cases, the surface alignment required to create a thermodynamically stable tilted CLC is a complex periodic pattern that cannot be obtained by rubbing. However, photoalignment techniques have been used to create a periodically varying alignment orientation pattern using the interference of two circularly polarized laser beams, and tilted helices have resulted when the period of the surface orientation is on the order of the pitch.[38,40] These volumetric diffractive gratings have been the subject of several recent studies.[38−42]

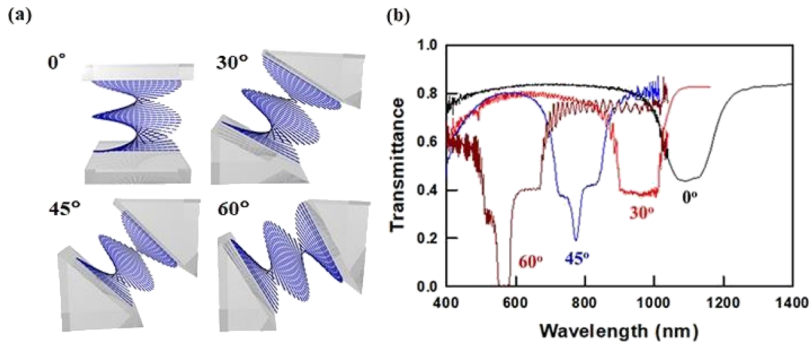

Figure 2. (a) Schematic illustrations of a planar CLC with light propagating at angles ψ of 0, 30, 45, and 60° relative to the helical axis. For angles other than 0°, pairs of glass prisms (graded light-gray regions) are used for approximate index matching and minimization of refraction at the glass−CLC interface. The light is incident from the top of each image (at normal incidence relative to the glass−air interface). (b) Transmission spectra of a planar CLC with a cell thickness of 18.8 μm and a pitch of ~700 nm taken at incidence angles ψ of 0, 30, 45, and 60° with unpolarized light.

https://dx.doi.org/10.1021/acsami.0c09845
ACS Appl. Mater. Interfaces 2020, 12, 37400−37408

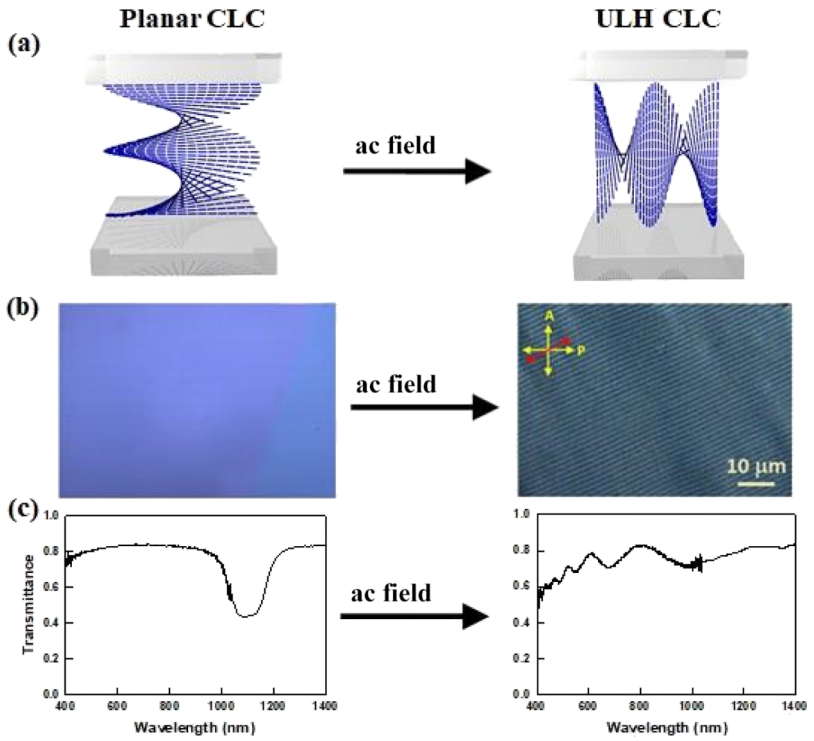

Figure 3. (a) Schematic illustration and (b) POM images of a planar CLC and ULH CLC. The pitch for the sample in (b) was 1470 nm, the cell thickness was 18.8 μm, and the ULH was obtained applying 15 V at 30 Hz. The red arrow in the right image in (b) indicates the rubbing direction; the yellow ones indicate the transmission axes of the polarizer and analyzer. (c) Transmission spectra of (left) a planar CLC and (right) ULH CLC sample at a normal angle of incidence relative to the substrate for unpolarized light. In (c), a cell thickness of 18.8 μm and a CLC with a pitch of ~700 nm were used, and 21 V at 30 Hz was applied in the ULH case.

In uniform lying helix (ULH) CLCs, the helical axis is in the plane of the substrate ($\mathbf{H} \perp \mathbf{N}$; see Figure 1b). Various methods have been reported to induce the ULH CLC conformation, including the application of electric fields through the thickness of the cell[43−45] often while slowly cooling the material from the isotropic phase[46] or shearing the sample;[47,48] the gradual decrease of the electric field amplitude starting from the homeotropic state of the material;[49] the preparation of scratches,[50] grooves, or polymer stripes[51] on the substrate; or the use of periodic alignment conditions imposed by photoalignment[52] or other photopatterning processes.[53,54] Short-pitched ULH CLCs ($L/P \gg 1$, where L is the cell thickness) have been obtained mainly by the electric field method with either high-frequency[49,55,56] or low-frequency[45] fields. The formation of the ULH CLC, its stability, and the presence of defects are dependent on several factors, including surface anchoring (alignment materials), applied electric field, pitch length, and cell thickness.[43,45] There is active research interest in exploiting their electro-optic, flexoelectric, and diffractive properties for a variety of applications.[52,57−60]

The mechanism of electrically induced orthogonal orientation switching of the CLC axis from the planar CLC ($\mathbf{H} \parallel \mathbf{N}$) to the ULH CLC ($\mathbf{H} \perp \mathbf{N}$) configuration is shown in Figure 3a. In this example, a low-frequency electric field was used, as in the case reported by Wang et al.[45] The switching of the helical axis orientation is enabled by an electric field of a moderate strength and a low frequency (~2−4 V/μm, 30 Hz) when the CLC has positive dielectric anisotropy. At low field strengths, the cell surface alignment dominates and the CLC remains in the planar state. At high field strengths, the director reorients parallel to the electric field, resulting in homeotropic alignment and loss of the helical structure, as typical. At intermediate voltages and low driving frequencies, it is possible to induce a ULH CLC alignment where the helical axis orients parallel to the cell substrate because of the electrohydrodynamic effect.[45] This electrically induced orthogonal orientation change can be seen in Figure 3b, which shows the polarized optical microscopy (POM) images of a planar homogeneous aligned CLC sample on the left and the electrically switched (~20 V, 30 Hz) ULH texture on the right side. The images in Figure 3b are obtained using a sample with a relatively long pitch length (P = 1.47 μm) so that striations associated with the modulation of the refractive index with periodicity along the helical axis can be resolved by optical microscopy. The texture in Figure 3b is characteristic of ULH CLCs with a pitch on the order of a micron or longer.[44,61] ULH CLCs with a shorter pitch typically appear of uniform color under cross polarizers and away from defects.[45,50,62] In Figure 3c, a conventional planar CLC sample probed at normal incidence ($\mathbf{H} \parallel \mathbf{N}$ and $\mathbf{k} \parallel \mathbf{N}$; see Figure 1a for definitions) with a notch at 1060 nm (50% transmittance) becomes transmissive upon electrically switching the helix orientation ($\mathbf{H} \perp \mathbf{N}$ and $\mathbf{H} \perp \mathbf{k}$; see Figure 1b). The transmission spectrum of the ULH CLC sample at normal incidence exhibits some oscillations, indicative of diffraction associated with the periodicity of the ULH CLC state in the direction perpendicular to the light propagation (Figure 3c, right).

ULH CLCs produced by the electrohydrodynamic approach are used here to investigate the angle dependence of the reflection color and polarization, and their relationship to those of planar CLCs. A switchable color change can be obtained by combining this helical orientation switching mechanism from

https://dx.doi.org/10.1021/acsami.0c09845
ACS Appl. Mater. Interfaces 2020, 12, 37400−37408

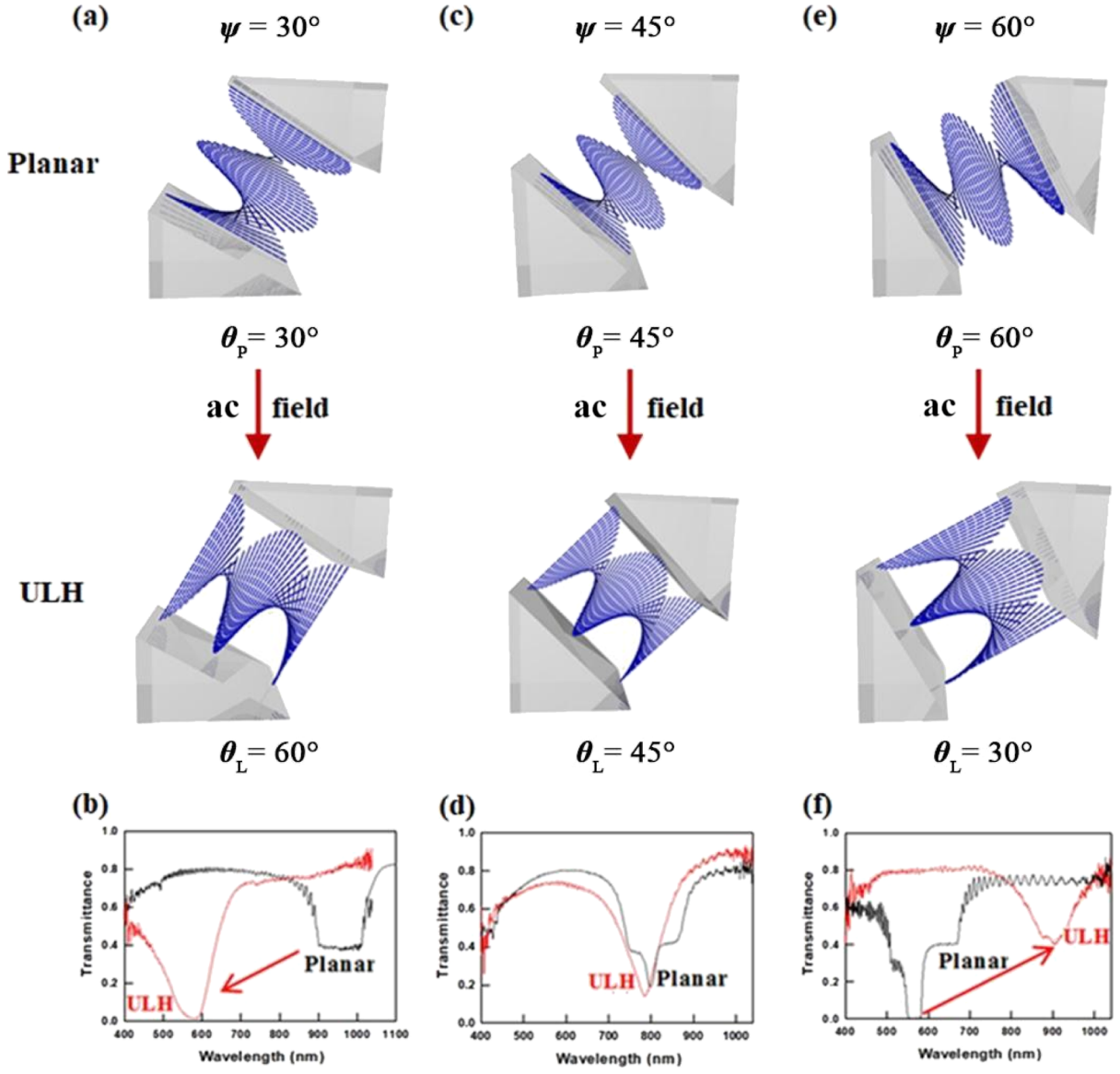

Figure 4. (a,c,e) Schematic diagrams and (b,d,f) transmission spectra of planar and ULH CLCs at oblique incidence angles ψ of (a,b) 30, (c,d) 45, and (e,f) 60°. The incident light is unpolarized. A voltage of 21 V (1.1 V/μm at 30 Hz) was applied to generate the ULH CLC and during the measurements for the ULH CLC case.

the planar CLC to the ULH CLC state with the inherent angular sensitivity of the Bragg wavelength in CLCs.

RESULTS AND DISCUSSION

For the investigation of the angle dependence of the transmission properties, the cells were mounted between prisms of various angles with an index-matching fluid as shown in Figure 1. In this configuration, the probe beam is normal to the top surface of the top prism, and the angle of incidence at the CLC−glass interface, ψ, is equal to the prism angle as the refractive indices of the glass and CLC medium are similar. Both the planar CLC and the ULH CLC states can be probed in this configuration at the same ψ. In the ULH CLC case, the angle between the incident light and the helical axis is $\theta_L = 90° - \psi$ (Figure 1b), whereas in the planar case, $\theta_P = \psi$ (Figure 1a). After electrically driving the ULH state, the helical axis **H** is oriented perpendicular to the surface alignment axis and in the substrate plane. It should be stated that for all the measurements discussed here, the cell was oriented so that the helical axis **H** of the ULH CLC was in the incidence plane. For the samples in this investigation, it was found that the helical axis of the ULH CLCs was perpendicular to the surface alignment direction. Thus, in Figure 1b, the surface alignment direction is pointing out of the page (see Figure S1 for a comparison of the behavior when **H** is in the incidence plane or perpendicular to it).

As shown in Figure 4a,b, for $\psi = 30°$, the planar CLC ($\theta_P = 30°$) shows a notch wavelength of 960 nm with ~50% transmission, while the ULH CLC ($\theta_L = 60°$) exhibits a transmission notch at 580 nm and high contrast (<1% transmission, unpolarized incident light). In the arrangement depicted in Figure 4c, where the cell substrate is tilted to 45° with respect to the incident light, the planar CLC ($\theta_P = 45°$) shows a band gap position of ~800 nm with ~20% transmittance (Figure 4d). The sample in the ULH orientation ($\theta_L = 45°$) shows a band in the same position but with a different shape (Figure 4d). When the cell substrate normal is tilted to 60° with respect to the incident light (Figure 4e), the

https://dx.doi.org/10.1021/acsami.0c09845
ACS Appl. Mater. Interfaces 2020, 12, 37400−37408

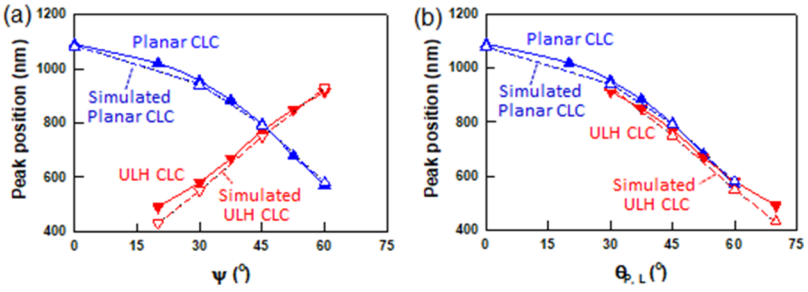

Figure 5. Summary of the experimental (filled symbols) and modeled (open symbols) transmission notch positions of the planar CLC and ULH CLC (a) at various incidence angles ψ and (b) as a function of θ_P and θ_L for the planar and ULH CLC orientations, respectively. The same samples as in Figure 4 (experimental data) and Figure S2 (modeled data) were used. An electric field of 1.1 V/μm (30 Hz) was applied during the measurements for the ULH CLC case.

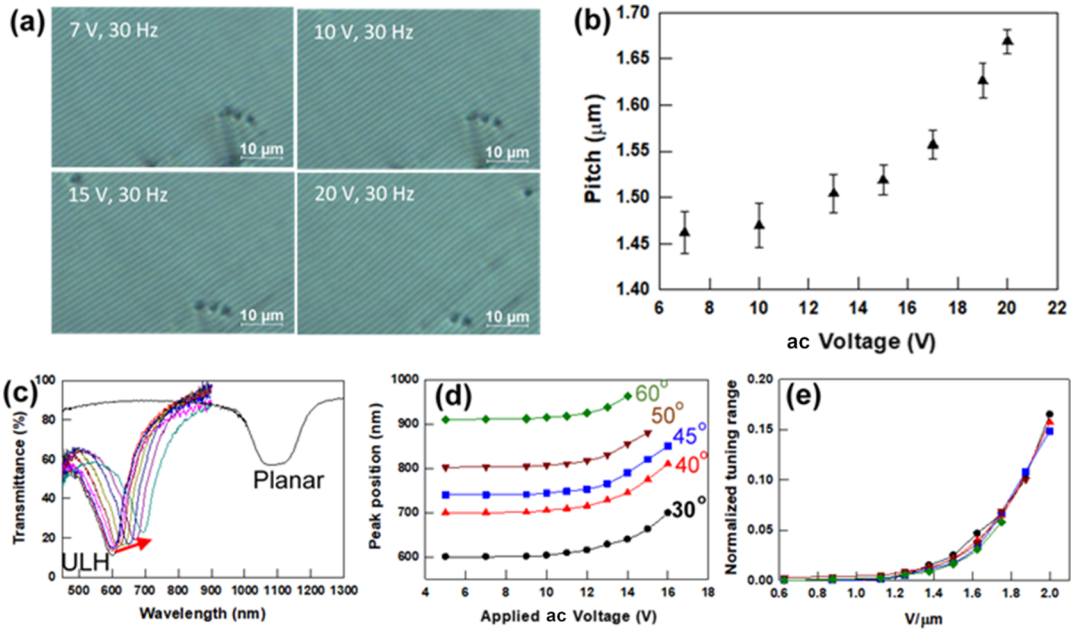

Figure 6. Electric field-controlled pitch in ULH CLCs: (a) POM images and (b) pitch change of a ULH CLC sample as a function of ac voltage. In (a,b), the pitch for the corresponding planar CLC is 1500 nm and the cell thickness is 8 μm. (c) Transmission spectra of a ULH CLC sample at ψ = 30°: upon increasing the voltage from 5 to 16 V at 30 Hz, the notch position shifts from 600 to about 700 nm (red arrow); the transmission spectrum for the corresponding planar CLC (at θ_P = 0°) is also shown; cell thickness = 8 μm; (d) notch wavelength position of the ULH CLC from graph (c) for various incidence angles and voltages and (e) normalized tuning range for each of the incidence angles as a function of electric field [same color legend as in (d)].

planar CLC (θ_P = 60°) exhibits a notch at ~575 nm and low transmittance (<1%), whereas upon electrically driving the ULH orientation (θ_L = 30°), the transmission notch red-shifts to ~900 nm and becomes circularly polarized (~50% transmission for unpolarized incident light), as is shown in the transmission spectra presented in Figure 4f. There is near equivalence in the transmission notch wavelength and polarization state (as estimated from the depth of the transmission band) of the planar CLC at ψ = 30° and the ULH CLC at ψ = 60° as for these θ_P = θ_L = 30°, and thus, the same Bragg wavelength λ_B is expected (eq 1). Similarly, the ULH CLC at ψ = 30° and the planar CLC at ψ = 60° have equivalent spectra (θ_P = θ_L = 60°). Specifically in both cases, the minimum transmittance is very low, a signature of unpolarized reflection. For ψ = 45°, θ_P = 45° and θ_L = 45°, and thus, no change in λ_B is expected (eq 1) when the CLC is switched from the planar to the ULH configuration, as is indeed observed in Figure 4d.

Modeling of light propagation in a liquid crystalline medium (see Figure S2 and the Experimental Section for details) was performed for a ULH CLC with P = 705 nm, a cell thickness of L = 18.8 μm, a nematic LC with refractive indices n_o = 1.52 and n_e = 1.73, and glass substrates with refractive index n_{glass} = 1.52. Refractive index dispersion and Fresnel reflections were neglected. As can be seen in Figure S2, the experimental and calculation results generally are in good agreement for the spectra calculated for the planar CLC and ULH CLC. The modeled spectra capture the main features of the experimental spectra; specifically, the wavelength position of the spectral notch shifts as the incidence angle is changed, which is in qualitative agreement with eq 1 and the experimental results. In addition, the transmittance at the center of the ULH CLC notch is significantly lower than 50% for ψ = 30 and 45° and increases with increasing ψ, as is the case experimentally. This supports the interpretation that the unpolarized regime of the CLC helix can be accessed in the ULH configuration for appropriate probing angles. The modeled transmission curves

https://dx.doi.org/10.1021/acsami.0c09845
ACS Appl. Mater. Interfaces 2020, 12, 37400−37408

have additional intricacies in the band shape that are not observed in the experimental spectra, which could be a result of the helical arrangement of the liquid crystal molecules in ULH CLCs being deformed from an ideal helix near the substrates because of the anchoring conditions imposed by the alignment layer,[44,61] which is not accounted for in the modeling. These deformations could also be responsible for the different band shapes observed experimentally for planar and ULH CLCs at the same angle θ (see Figure 4b,d,f). In addition, in the ULH CLC configuration, there is a local periodic variation of the refractive index at the CLC−glass interface because **H** is in the plane of the substrate. This index modulation could lead to refractive effects that are not present in the case of planar CLCs, where the refractive index experienced by the incident beam is the same across the beam profile.

The transmission notch wavelengths in the planar CLC and the ULH CLC state for the same sample are summarized in Figure 5a as a function of incidence angle ψ. As discussed earlier, the band gap of the planar CLCs blue-shifts as the angle of incidence increases (see Figure 2b and the blue line in Figure 5b), whereas the transmission notch in the ULH CLCs red-shifts with increasing incidence angle, as shown by the red line in Figure 5a. When these data are reported as a function of θ_P and θ_L, the two curves almost overlap (see Figure 5b), given the relationship described earlier between these angles, and follow approximately the trend of eq 1. The data in Figure 5b also suggest that the underlying pitch is the same for the planar and ULH CLC states of the sample (under the experimental conditions used here, the effect of the electric field on the pitch was negligible, as discussed below).

Lavrentovich and colleagues investigated the behavior of ULH CLC samples exhibiting Bragg or Raman−Nath diffraction.[43,44] For cells with $L/P > 1$ (where L is the cell thickness), the diffraction angle was found to depend on the applied voltage for voltage magnitudes larger than the reorienting threshold. This change was associated with a pitch increase as a result of the progressive unwinding of the CLC helix by the electric field until, at a high field, the LC molecules align along the electric field (homeotropic state) and the cell becomes transparent.[44,45,61,62] An example of this pitch length increase in a ULH CLC with ac voltage is shown in Figure 6a,b, where the pitch changes from 1.46 to 1.67 μm when the applied voltage is increased from 7 to 20 V. The pitch change in Figure 6b is consistent with the one previously observed in the literature for ULH CLCs,[44,61] which in turn is similar to the helix unwinding behavior of an unbound CLC in an electric field.[63]

Exploiting this field-induced pitch change, the ULH CLC devices described above can be made electrically tunable for any of the probing angles. Figure 6c shows the transmission spectra of a CLC cell at $\psi = 30°$. The planar CLC before the application of the electric field shows a notch at 1080 nm. The notch position shifts to ~600 nm when the ULH CLC is produced by applying a low voltage (5 V, 0.625 V/μm), and it shifts by about 100 nm to the red when the voltage is increased to 16 V (2.0 V/μm). Red shifting of the ULH CLC transmission notch wavelength is seen for all angles of incidence (Figure 6d). It can also be seen from Figure 6d that there is almost no change in peak position below 9 V. The experimental results in Figures 4 and 5 were obtained with voltages in the corresponding flat regime for each of the samples so that the field-induced pitch elongation was negligible. The tuning ranges for the planar CLC and ULH CLC are equivalent once normalized to the starting position for each angle (Figure 6e), as expected for a tuning process associated with the field-induced pitch dilation. Thus, a tuning range of about 15% can be obtained in ULH CLC devices before they become unstable at high fields.

CONCLUSIONS

In this study, we report CLC devices with an electrically switchable color. The devices exploit the electrical reorientation of the helical axis from perpendicular to the cell substrate (planar CLC) to parallel to the substrate (ULH CLC). When the cells are probed away from the substrate normal, both states exhibit selective coloration. The direction of color change (red or blue shift) as a result of the helix reorientation from planar to ULH depends on the incidence angle. In addition, for the probing geometry used here, at least one of the two states is characterized by an unpolarized transmission notch. This characteristic and the fact that the ULH CLC color can be electrically tuned over approximately 15% of the notch position provide the devices with properties that are hard to achieve in other LC configurations. This study provides a new perspective on ULH CLCs, which have previously mainly been studied as diffraction gratings[43,44,58,64] or to exploit the flexoelectric effect.[46,47] The use of prisms to access various incidence angles brings to light the complementarity of behavior between ULH and planar CLCs.

This work suggests that the reconfigurability of CLCs can be exploited in a different way by using ULH CLCs as the material platform and oblique incidences for probing of their optical properties. As discussed in the Introduction, the polarization state and center wavelength of the selective reflection from CLCs depend on the angle of incidence.[27,29,35,65] This work suggests a device geometry that allows to access this effect in both the planar and ULH CLC configurations on the same physical sample. The device can be switched by applying an electric field between the top and bottom electrodes, and both states are reflective for any prism or any incidence angle $\psi > 0°$. The lengthening of the cholesteric pitch and unwinding of the helix in the presence of an electric field directed along the helical axis were used to achieve tuning of the Bragg reflection band using uniform top and bottom electrodes and a ULH CLC probed at oblique incidence. The reconfigurable polarization and angular chromaticity of these materials are particularly promising for 3D display applications where controlling the properties of light as a function of angle is important to transmit different perspectives to each eye.

EXPERIMENTAL SECTION

Preparation of Cells and Planar and ULH CLCs. Alignment cells were prepared from indium tin oxide-coated glass slides (Colorado Concept Coatings LLC). The substrates were then cleaned in acetone and methanol and treated with air plasma. The substrates were subsequently coated with a polyimide alignment layer (PI2555, HD Microsystems) and rubbed with velvet. The cell gap was controlled by mixing glass rod spacers into an optical adhesive, and it was measured using an optical interference method. CLC samples were prepared by mixing right-handed chiral dopants (CB15 and/or R1011, Merck) and a positive $\Delta\varepsilon$ nematic LC (E7, T_{NI} = 58 °C, $\Delta\varepsilon$ = 13.8, birefringence Δn = 0.2253, and average refractive index $\langle n \rangle = (n_e + 2n_o)/3$ = 1.5937 at λ = 589 nm and 20 °C, Merck). All materials were used as received without any purification. The ULH CLC samples were prepared by application of ac voltages at a low frequency

https://dx.doi.org/10.1021/acsami.0c09845
ACS Appl. Mater. Interfaces 2020, 12, 37400−37408

(30 Hz) to the planar CLC samples. Once the ULH state was formed, no instabilities were observed in the samples if the low-frequency voltage was applied continuously for periods on the order of 60 min. The samples did not exhibit an electric field dependence of the orientation of the ULH CLC helical axis of the type reported by Lee and Patel[55] or by Salter et al.[66] (dependence on $1/E$, where E is the electric field). The difference could arise from the type of alignment layers in use. The rotation of the helical axis due to the flexoelectric effect is expected to be small for the samples used in this study (see the Supporting Information).

Experimental Setup and Measurements. Transmission spectra were recorded with a fiber optic spectrometer (resolution ~ 1.5 nm). Measurements at oblique angles of incidence relative to the cell substrate were performed by mounting the cell between Littrow or right angle prisms (Edmund Optics) and using mineral oil (refractive index = 1.467, Sigma-Aldrich) as an index-matching fluid between the cell and the prisms. Additional incidence angles were accessed by immersing the sample in a home-made quartz box filled with the mineral oil. Unpolarized light was used as the probe beam. Transmission spectra were recorded before, during, and after the application of ac fields. The spectra have not been corrected for reflection losses. It should be mentioned that observing the sample at oblique incidence while applying moderate fields allowed for an easy determination of the threshold voltage necessary to induce the ULH CLC state.

Modeling of Light Propagation in CLCs. COMSOL Multiphysics software was used. The modeling domain included a CLC in the ULH or planar configuration placed between two glass substrates and bounded by perfectly matched layers. Fresnel reflections were neglected. The transmittance for transverse-magnetic and transverse-electric polarized light was calculated separately and then combined to obtain the transmittance for unpolarized light. The results for the planar and ULH CLCs are shown in Figure S2a,b, respectively. The spectra in Figure S2 have been scaled to have, approximately, the same off-band transmittance ($T \sim 0.8$) as the experimental spectra, which are affected by reflection and scattering losses.

■ ASSOCIATED CONTENT

Supporting Information

The Supporting Information is available free of charge at https://pubs.acs.org/doi/10.1021/acsami.0c09845.

> Schematic of ULH CLCs and transmission spectra for two orientations of the helical axis, **H**, relative to the incidence plane; calculated transmission spectra for a planar CLC and ULH CLC for various incidence angles and comparison with experimental results; and estimate of the axis tilt due to the flexoelectric effect (PDF)

■ AUTHOR INFORMATION

Corresponding Author

Michael E. McConney − *Air Force Research Laboratory, Materials and Manufacturing Directorate, Wright-Patterson AFB, Ohio 45433, United States;* orcid.org/0000-0002-6249-6836; Email: Michael.Mcconney.1@us.af.mil

Authors

Kyung Min Lee − *Air Force Research Laboratory, Materials and Manufacturing Directorate, Wright-Patterson AFB, Ohio 45433, United States; Azimuth Corporation, Fairborn, Ohio 45324, United States*

Mariacristina Rumi − *Air Force Research Laboratory, Materials and Manufacturing Directorate, Wright-Patterson AFB, Ohio 45433, United States; Azimuth Corporation, Fairborn, Ohio 45324, United States;* orcid.org/0000-0002-4597-9617

Matthew S. Mills − *Air Force Research Laboratory, Materials and Manufacturing Directorate, Wright-Patterson AFB, Ohio 45433, United States*

Victor Reshetnyak − *Theoretical Physics Department, Taras Shevchenko National University of Kyiv, Kyiv 01601, Ukraine*

Dean R. Evans − *Air Force Research Laboratory, Materials and Manufacturing Directorate, Wright-Patterson AFB, Ohio 45433, United States*

Timothy J. Bunning − *Air Force Research Laboratory, Materials and Manufacturing Directorate, Wright-Patterson AFB, Ohio 45433, United States*

Complete contact information is available at: https://pubs.acs.org/10.1021/acsami.0c09845

Notes

The authors declare no competing financial interest.

■ ACKNOWLEDGMENTS

The authors acknowledge funding from the Materials and Manufacturing Directorate of the Air Force Research Laboratory, Wright-Patterson Air Force Base, under contract #FA8650-16-D-5404-0009. The authors would like to thank Vincent Tondiglia for support with the optical setups used for the characterization, Ecklin Crenshaw for help with schematic images, and Dr. Ighodalo Idehenre and Dr. Benjamin Kowalski for helpful discussions on this work.

■ REFERENCES

(1) Livingstone, M.; Hubel, D. Segregation of Form, Color, Movement, and Depth: Anatomy Physiology and Perception. *Science* **1988**, *240*, 740−749.

(2) Westheimer, G. The Ferrier Lecture, 1992. Seeing Depth with Two Eyes: Stereopsis. *Proc. R. Soc. London, Ser. B* **1994**, *257*, 205−214.

(3) Kitzerow, H.-S.; Bahr, C. *Chirality in Liquid Crystals*; Springer-Verlag: New York, 2001.

(4) Wu, S. T.; Yang, D.-K. *Reflective Liquid Crystal Displays*; Wiley: West Sussex, UK, 2001.

(5) de Gennes, P. G.; Prost, J. *The Physics of Liquid Crystals*; Clarendon Press: Oxford, 1993.

(6) Huang, Y.; Zhou, Y.; Doyle, C.; Wu, S.-T. Tuning the Photonic Band Gap in Cholesteric Liquid Crystals by Temperature-dependent Dopant Solubility. *Opt. Express* **2006**, *14*, 1236.

(7) Natarajan, L. V.; Wofford, J. M.; Tondiglia, V. P.; Sutherland, R. L.; Koerner, H.; Vaia, R. A.; Bunning, T. J. Electro-thermal Tuning in a Negative Dielectric Cholesteric Liquid Crystal Material. *J. Appl. Phys.* **2008**, *103*, 093107.

(8) McConney, M. E.; Tondiglia, V. P.; Hurtubise, J. M.; Natarajan, L. V.; White, T. J.; Bunning, T. J. Thermally Induced, Multicolored Hyper-Reflective Cholesteric Liquid Crystals. *Adv. Mater.* **2011**, *23*, 1453−1457.

(9) White, T. J.; McConney, M. E.; Bunning, T. J. Dynamic color in stimuli-responsive cholesteric liquid crystals. *J. Mater. Chem.* **2010**, *20*, 9832.

(10) Bisoyi, H. K.; Li, Q. Light-driven Liquid Crystalline Materials: From Photo-induced Phase Transitions and Property Modulations to Applications. *Chem. Rev.* **2016**, *116*, 15089−15166.

(11) Zola, R. S.; Bisoyi, H. K.; Wang, H.; Urbas, A. M.; Bunning, T. J.; Li, Q. Dynamic Control of Light Direction Enabled by Stimuli-Responsive Liquid Crystal Gratings. *Adv. Mater.* **2019**, *31*, 1806172.

(12) Yuan, C.-L.; Huang, W.; Zheng, Z.-g.; Liu, B.; Bisoyi, H. K.; Li, Y.; Shen, D.; Lu, Y.; Li, Q. Stimulated Transformation of Soft Helix Among Helicoidal, Heliconical, and Their Inverse Helices. *Sci. Adv.* **2019**, *5*, eaax9501.

(13) Bisoyi, H. K.; Bunning, T. J.; Li, Q. Stimuli-Driven Control of the Helical Axis of Self-Organized Soft Helical Superstructures. *Adv. Mater.* **2018**, *30*, 1706512.
(14) Wang, L.; Bisoyi, H. K.; Zheng, Z.; Gutierrez-Cuevas, K. G.; Singh, G.; Kumar, S.; Bunning, T. J.; Li, Q. Stimuli-directed Self-organized Chiral Superstructures for Adaptive Windows Enabled by Mesogen-functionalized Graphene. *Mater. Today* **2017**, *20*, 230.
(15) Hikmet, R. A. M.; Kemperman, H. Electrically Switchable Mirrors and Optical Components Made from Liquid-crystal Gels. *Nature* **1998**, *392*, 476−479.
(16) Xianyu, H.; Faris, S.; Crawford, G. P. In-plane Switching of Cholesteric Liquid Crystals for Visible and Near-infrared Applications. *Appl. Opt.* **2004**, *43*, 5006−5015.
(17) Lin, T.-H.; Jau, H.-C.; Chen, C.-H.; Chen, Y.-J.; Wei, T.-H.; Chen, C.-W.; Fuh, A. Y.-G. Electrically Controllable Laser based on Cholesteric Liquid Crystal with Negative Dielectric Anisotropy. *Appl. Phys. Lett.* **2006**, *88*, 061122.
(18) White, T. J.; Bricker, R. L.; Natarajan, L. V.; Tondiglia, V. P.; Green, L.; Li, Q.; Bunning, T. J. Electrically Switchable, Photo-addressable Cholesteric Liquid Crystal Reflectors. *Opt. Express* **2010**, *18*, 173.
(19) McConney, M. E.; Tondiglia, V. P.; Natarajan, L. V.; Lee, K. M.; White, T. J.; Bunning, T. J. Electrically Induced Color Changes in Polymer-stabilized Cholesteric Liquid Crystals. *Adv. Opt. Mater.* **2013**, *1*, 417−421.
(20) McConney, M. E.; Tondiglia, V. P.; Hurtubise, J. M.; White, T. J.; Bunning, T. J. Photoinduced Hyper-reflective Cholesteric Liquid Crystals enabled *via* Surface Initiated Photopolymerization. *Chem. Commun.* **2011**, *47*, 505−507.
(21) Mitov, M.; Dessaud, N. Going Beyond the Reflectance Limit of Cholesteric Liquid Crystals. *Nat. Mater.* **2006**, *5*, 361.
(22) Tasolamprou, A. C.; Mitov, M.; Zografopoulos, D. C.; Kriezis, E. E. Theoretical and Experimental Studies of Hyperreflective Polymer-network Cholesteric Liquid Crystal Structures with Helicity Inversion. *Opt. Commun.* **2009**, *282*, 903−907.
(23) Guo, J.; Cao, H.; Wei, J.; Zhang, D.; Liu, F.; Pan, G.; Zhao, D.; He, W.; Yang, H. Polymer Stabilized Liquid Crystal Films Reflecting both Right- and Left-circularly Polarized Light. *Appl. Phys. Lett.* **2008**, *93*, 201901.
(24) Agez, G.; Mitov, M. Cholesteric Liquid Crystalline Materials with a Dual Circularly Polarized Light Reflection Band Fixed at Room Temperature. *J. Phys. Chem. B* **2011**, *115*, 6421−6426.
(25) Mitov, M. Cholesteric Liquid Crystals with a Broad Light Reflection Band. *Adv. Mater.* **2012**, *24*, 6260−6276.
(26) Fergason, J. L. Cholesteric Structure-1 Optical Properties. *Mol. Cryst.* **1966**, *1*, 293.
(27) Belyakov, V. A.; Dmitrienko, V. E. Theory of the Optical Properties of Cholesteric Liquid Crystals. *Sov. Phys. Solid State* **1974**, *15*, 1811.
(28) Belyakov, V. A.; Dmitrienko, V. E.; Orlov, V. P. Optics of Cholesteric Liquid Crystals. *Sov. Phys. Usp.* **1979**, *22*, 64−88.
(29) Takezoe, H.; Ouchi, Y.; Hara, M.; Fukuda, A.; Kuze, E. Experimental Studies on Reflection Spectra in Monodomain Cholesteric Liquid Crystal Cells: Total Reflection, Subsidiary Oscillation and Its Beat or Swell Structure. *Jpn. J. Appl. Phys.* **1983**, *22*, 1080.
(30) Takezoe, H.; Ouchi, Y.; Sugita, A.; Hara, M.; Fukuda, A.; Kuze, E. Experimental Observation of the Total Reflection by a Monodomain Cholesteric Liquid Crystal. *Jpn. J. Appl. Phys.* **1982**, *21*, L390.
(31) Kralik, J. C.; Vithana, H.; Tripathi, S.; Faris, S. M. Polarization Crosstalk in CLC Films at Oblique Angles of Incidence. *Mol. Cryst. Liq. Cryst.* **1997**, *301*, 307.
(32) Huck, N. P. M.; Staupe, I.; Thirouard, A.; de Boer, D. K. G. Light Polarization by Cholesteric Layers. *Jpn. J. Appl. Phys.* **2003**, *42*, 5189−5194.
(33) Gevorgyan, A. H. Effects of Angle of Incidence and Polarization in the Chiral Photonic Crystals. *Opt. Spectrosc.* **2008**, *105*, 624−632.
(34) Umanskii, B. A.; Simdyankin, I. V. Angular Dependences of Transmission Spectra of Chiral Liquid Crystals. *Crystallogr. Rep.* **2017**, *62*, 448−454.
(35) Ozaki, R. Simple Model for Estimating Band Edge Wavelengths of Selective Reflection from Cholesteric Liquid Crystals for Oblique Incidence. *Phys. Rev. E* **2019**, *100*, 012708.
(36) Rafayelyan, M. S.; Gharagulyan, H.; Sarukhanyan, T. M.; Gevorgyan, A. H.; Hakobyan, R. S.; Alaverdyan, R. B. Light Energy Accumulation by Cholesteric Liquid Crystal Layer at Oblique Incidence. *Liq. Cryst.* **2019**, *46*, 1079−1090.
(37) Tondiglia, V. P.; Rumi, M.; Idehenre, I. U.; Lee, K. M.; Binzer, J. F.; Banerjee, P. P.; Evans, D. R.; McConney, M. E.; Bunning, T. J.; White, T. J. Electrical Control of Unpolarized Reflectivity in Polymer-Stabilized Cholesteric Liquid Crystals at Oblique Incidence. *Adv. Opt. Mater.* **2018**, *6*, 1800957.
(38) Nys, I.; Stebryte, M.; Ussembayev, Y. Y.; Beeckman, J.; Neyts, K. Tilted Chiral Liquid Crystal Gratings for Efficient Large-Angle Diffraction. *Adv. Opt. Mater.* **2019**, *7*, 1901364.
(39) Xiong, J.; Chen, R.; Wu, S.-T. Device Simulation of Liquid Crystal Polarization Gratings. *Opt. Express* **2019**, *27*, 18102−18112.
(40) Lee, Y.-H.; Yin, K.; Wu, S.-T. Reflective Polarization Volume Gratings for High Efficiency Waveguide-coupling Augmented Reality Displays. *Opt. Express* **2017**, *25*, 27008−27014.
(41) Xiang, X.; Kim, J.; Komanduri, R.; Escuti, M. J. Nanoscale Liquid Crystal Polymer Bragg Polarization Gratings. *Opt. Express* **2017**, *25*, 19298−19308.
(42) Lee, Y.-H.; He, Z.; Wu, S.-T. Optical Properties of Reflective Liquid Crystal Polarization Volume Gratings. *J. Opt. Soc. Am. B* **2019**, *36*, D9−D12.
(43) Subacius, D.; Bos, P. J.; Lavrentovich, O. D. Switchable diffractive cholesteric gratings. *Appl. Phys. Lett.* **1997**, *71*, 1350.
(44) Subacius, D.; Shiyanovskii, S. V.; Bos, P.; Lavrentovich, O. D. Cholesteric Gratings with Field-controlled Period. *Appl. Phys. Lett.* **1997**, *71*, 3323.
(45) Wang, C.-T.; Wang, W.-Y.; Lin, T.-H. A Stable and Switchable Uniform Lying Helix Structure in Cholesteric Liquid Crystals. *Appl. Phys. Lett.* **2011**, *99*, 041108.
(46) Patel, J. S.; Meyer, R. B. Flexoelectric Electro-optics of a Cholesteric Liquid Crystal. *Phys. Rev. Lett.* **1987**, *58*, 1538−1540.
(47) Rudquist, P.; Buivydas, M.; Komitov, L.; Lagerwall, S. T. Linear electro-optic effect based on flexoelectricity in a cholesteric with sign change of dielectric anisotropy. *J. Appl. Phys.* **1994**, *76*, 7778−7783.
(48) Inoue, Y.; Moritake, H. Formation of a Defect-free Uniform Lying Helix in a Thick Cholesteric Liquid Crystal Cell. *Appl. Phys. Express* **2015**, *8*, 071701.
(49) Yu, C.-H.; Wu, P.-C.; Lee, W. Alternative Generation of Well-aligned Uniform Lying Helix Texture in a Cholesteric Liquid Crystal Cell. *AIP Adv.* **2017**, *7*, 105107.
(50) Outram, B. I.; Elston, S. J. Spontaneous and Stable Uniform Lying Helix Liquid-crystal Alignment. *J. Appl. Phys.* **2013**, *113*, 043103.
(51) Carbone, G.; Salter, P.; Elston, S. J.; Raynes, P.; De Sio, L.; Ferjani, S.; Strangi, G.; Umeton, C.; Bartolino, R. Short pitch cholesteric electro-optical device based on periodic polymer structures. *Appl. Phys. Lett.* **2009**, *95*, 011102.
(52) Ma, L.-L.; Li, S.-S.; Li, W.-S.; Ji, W.; Luo, B.; Zheng, Z.-G.; Cai, Z.-P.; Chigrinov, V.; Lu, Y.-Q.; Hu, W.; Chen, L.-J. Rationally Designed Dynamic Superstructures Enabled by Photoaligning Cholesteric Liquid Crystals. *Adv. Opt. Mater.* **2015**, *3*, 1691−1696.
(53) Komitov, L.; Bryan-Brown, G. P.; Wood, E. L.; Smout, A. B. J. Alignment of Cholesteric Liquid Crystals using Periodic Anchoring. *J. Appl. Phys.* **1999**, *86*, 3508−3511.
(54) Hegde, G.; Komitov, L. Periodic anchoring condition for alignment of a short pitch cholesteric liquid crystal in uniform lying helix texture. *Appl. Phys. Lett.* **2010**, *96*, 113503.
(55) Lee, S.-D.; Patel, J. S. Surface Effect on the Field-induced Structural Change near the Isotropic-cholesteric Transition. *Phys. Rev. A* **1990**, *42*, 997−1000.

https://dx.doi.org/10.1021/acsami.0c09845
ACS Appl. Mater. Interfaces 2020, 12, 37400−37408

(56) Salter, P. S.; Kischka, C.; Elston, S. J.; Raynes, E. P. The Influence of Chirality on the Difference in Flexoelectric Coefficients Investigated in Uniform Lying Helix, Grandjean and Twisted Nematic Structures. *Liq. Cryst.* **2009**, *36*, 1355−1364.
(57) Zheng, Z.-g.; Li, Y.; Bisoyi, H. K.; Wang, L.; Bunning, T. J.; Li, Q. Three-dimensional Control of the Helical Axis of a Chiral Nematic Liquid Crystal by Light. *Nature* **2016**, *531*, 352−356.
(58) Zhang, L.; Wang, L.; Hiremath, U. S.; Bisoyi, H. K.; Nair, G. G.; Yelamaggad, C. V.; Urbas, A. M.; Bunning, T. J.; Li, Q. Dynamic Orthogonal Switching of a Thermoresponsive Self-organized Helical Superstructure. *Adv. Mater.* **2017**, *29*, 1700676.
(59) Ryabchun, A.; Bobrovsky, A.; Stumpe, J.; Shibaev, V. Electroinduced Diffraction Gratings in Cholesteric Polymer with Phototunable Helix Pitch. *Adv. Opt. Mater.* **2015**, *3*, 1462−1469.
(60) Ryabchun, A.; Bobrovsky, A. Cholesteric Liquid Crystal Materials for Tunable Diffractive Optics. *Adv. Opt. Mater.* **2018**, *6*, 1800335.
(61) Shiyanovskii, S. V.; Subacius, D.; Voloschenko, D.; Bos, P. J.; Lavrentovich, O. D. Cholesteric Diffraction Devices with a Field-controlled Grating Vector. *SPIE's International Symposium on Optical Science, Engineering, and Instrumentation*, 1998; Vol. *3475*, pp 56−64.
(62) Park, K.-S.; Baek, J.-H.; Lee, Y.-J.; Kim, J.-H.; Yu, C.-J. Effects of Pretilt Angle and Anchoring Energy on Alignment of Uniformly Lying Helix Mode. *Liq. Cryst.* **2016**, *43*, 1184−1189.
(63) de Gennes, P. G. Calcul de la distorsion d'une structure cholesterique par un champ magnetique. *Solid State Commun.* **1968**, *6*, 163−165.
(64) Fuh, A. Y.-G.; Lin, C.-H.; Huang, C.-Y. Dynamic Pattern Formation and Beam-steering Characteristics of Cholesteric Gratings. *Jpn. J. Appl. Phys.* **2002**, *41*, 211−218.
(65) Risse, A. M.; Schmidtke, J. Angular-Dependent Spontaneous Emission in Cholesteric Liquid-Crystal Films. *J. Phys. Chem. C* **2019**, *123*, 2428−2440.
(66) Salter, P. S.; Elston, S. J.; Raynes, P.; Parry-Jones, L. A. Alignment of the Uniform Lying Helix Structure in Cholesteric Liquid Crystals. *Jpn. J. Appl. Phys.* **2009**, *48*, 101302.

https://dx.doi.org/10.1021/acsami.0c09845
ACS Appl. Mater. Interfaces 2020, 12, 37400−37408